Materials Horizons

ROYAL SOCIETY OF CHEMISTRY

REVIEW

View Article Online
View Journal | View Issue



Cite this: *Mater. Horiz.*, 2021, **8**, 1618

# Polydopamine antibacterial materials

Yu Fu,[a] Lei Yang,[a] Jianhua Zhang,[a] Junfei Hu,[a] Gaigai Duan,[b] Xianhu Liu,[c] Yiwen Li*[a] and Zhipeng Gu*[a]

Received 13th December 2020,
Accepted 26th January 2021

DOI: 10.1039/d0mh01985b

rsc.li/materials-horizons

Recently, the development of polydopamine (PDA) has demonstrated numerous excellent performances in free radical scavenging, UV shielding, photothermal conversion, and biocompatibility. These unique properties enable PDA to be widely used as efficient antibacterial materials for various applications. Accordingly, PDA antibacterial materials mainly include free-standing PDA materials and PDA-based composite materials. In this review, an overview of PDA antibacterial materials is provided to summarize these two types of antibacterial materials in detail, including the fabrication strategies and antibacterial mechanisms. The future development and challenges of PDA in this field are also presented. It is hoped that this review will provide an insight into the future development of antibacterial functional materials based on PDA.



## 1 Introduction

As a type of tiny ancient creature, bacteria have great influences on the daily life of humans. Other than some beneficial probiotics, most bacteria cause infectious diseases and pose a threat to human health.[1] Besides, bacterial infections and related diseases caused by implanted devices may interfere with healthcare and clinical treatment.[2,3] Antibiotics have been the earliest drug used for sterilization and the discovery of penicillin has gradually eliminated diseases such as phthisis. However, antibiotic abuse causes bacterial resistance, and antibiotics are insalubrious due to certain damage to the liver and nervous system, causing serious influence on hearing, eyesight, *etc.*[4,5] Therefore, many other antibacterial agents such as quaternary ammonium salts (QAS), metal ions, antimicrobial peptides, graphene oxide (GO) sheet, and nitric oxide (NO) have been gradually developed and have exhibited excellent antibacterial effects.[6] However, they also have some deficiencies. For example, QAS also lack bacterial resistance.[7] Metal ions/oxides have broad-spectrum antibacterial properties but the uncontrolled release of ions, limited application, and significant cytotoxicity limit the widespread employment of these materials.[8,9] Although, new antimicrobial materials, such as carbon nanotubes (CNTs) and GO, have been extensively studied, their public safety and environmental impacts have not been thoroughly assessed.[10] In view of the above reasons, it is still necessary to develop novel materials with safe, efficient, and controllable antibacterial effects. Meanwhile, the preparation process of materials needs to be simpler and more convenient, which is more conducive for the popularization and promotion of materials.

Polydopamine (PDA) is a mussel-inspired material derived from mussel adhesive proteins with strong wet adhesion to substrates. Since the first report in 2007,[11] PDA has been widely used for biomaterials,[12–15] energy and catalysts,[16] and other fields.[17–19] It is mainly due to the outstanding performances of PDA, *e.g.*, in radical scavenging, ultraviolet shielding, photothermal conversion, electrochemical and biocompatible performances, which are credited to its hierarchical chemical and physical properties.[20,21] Specifically, catechol and primary amine groups endow PDA with excellent adhesion, metal coordination, and antioxidant capacity.[22–24] Similar to many natural polyphenols with catechol structures that can be used as building blocks of biomaterials through their metal chelation effect and various chemical reactions, the catechols in PDA provide efficient modification sites.[25–31] The indole structures and various non-covalent interactions (*e.g.*, π–π, cation–π, and hydrogen bonding interactions) make PDA form a large number of planar conjugated structures and donor–acceptor structures, and possess a wide spectrum of absorption, excellent photothermal conversion, and electrochemical performances.[32–35] Based on its inherent properties, PDA has gradually become a potential antibacterial material. On the one hand, excellent photothermal conversion ability, rich catechols, and secondary amine structures, and the hydrogen peroxide formed by PDA can denature the protein of the cell membrane, destroying the

[a] *College of Polymer Science and Engineering, State Key Laboratory of Polymer Materials Engineering, Sichuan University, Chengdu, Sichuan 610065, China. E-mail: guzhipeng2019@scu.edu.cn, ywli@scu.edu.cn; Tel: +86 028-85401066, +86 028-85401066*

[b] *Co-Innovation Center of Efficient Processing and Utilization of Forest Resources, College of Materials Science and Engineering, Nanjing Forestry University, Nanjing 210037, China*

[c] *National Engineering Research Center for Advanced Polymer Processing Technology, Zhengzhou University, Zhengzhou 450002, China*

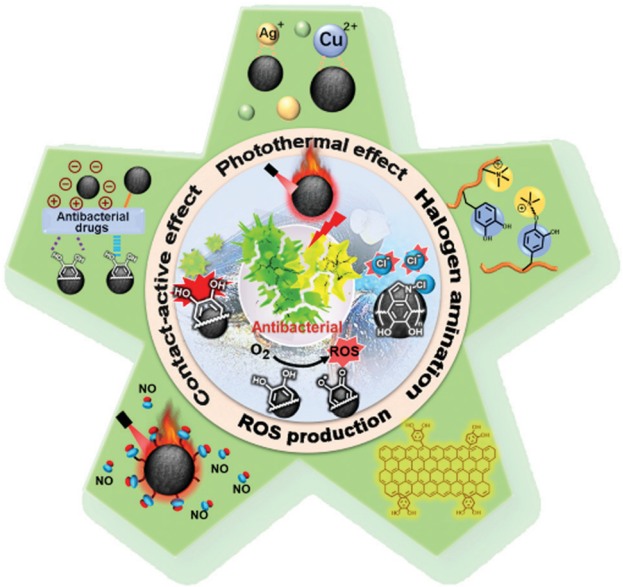


Scheme 1 Overview of the fabrication strategies and antibacterial mechanisms of PDA antibacterial materials.

Table 1 Summary of antibacterial behaviors of PDA materials with different mechanisms

| Antibacterial mechanism | Bacteria | Effect | Ref. |
|---|---|---|---|
| Contact-active | *E. coli* | 49% | 42 |
| | *E. coli* | Effective | 48 |
| | *E. coli* | ≥90% | 36 |
| | *S. aureus* | ≥95% | |
| | *P. aeruginosa* | ≥95% | |
| PTT | *E. coli* | 97% | 50 |
| | *S. aureus* | 98.4% | |
| | *C. albicans* | 98.7% | |
| | *S. aureus* | ~92.3% | 38 |
| | *E. coli* | Effective | 37 |
| | *S. aureus* | | |
| ROS induce | *E. coli* | ~100% | 39 |
| | *S. aureus* | | |
| | MRSA | | |
| | *P. aeruginosa* | | |
| | MRSA | ~100% | 53 |
| | *E. coli* | | |
| Halogen amination | *E. coli* | Effective | 45 |
| | *S. aureus* | | |

structure of the bacterial cell membrane and causing the death of the bacteria, which makes PDA an innovative and highly effective biological antibacterial agent.[36–39] On the other hand, thanks to the abundant chemical reaction sites and the gentle preparation strategy, PDA was widely used in the interface chemical modification of antibacterial composite materials.[40] For example, silver ions ($Ag^+$) can grow into antibacterial Ag nanoparticles (Ag NPs) *in situ* on the surface of PDA to build an antibacterial interface.[41]

The purpose of this review is to summarize the fabrication strategies and antibacterial mechanisms of PDA-based antibacterial materials (Scheme 1). In the first section, we discuss the antibacterial effects and mechanisms of PDA as a freestanding antibacterial material. In the second section, we focus on a variety of functional antibacterial composite materials with excellent antibacterial performances assisted by PDA, which include PDA–Ag NPs, copper ions ($Cu^{2+}$), antibacterial drugs, QAS, CNMs, and NO. Finally, the summary and prospects of PDA-based antibacterial materials are proposed. We hope that this review will play a positive role in promoting the design and fabrication of antibacterial materials in the future.

## 2 Freestanding PDA antibacterial materials

Benefitting from its unique antibacterial ability, good biocompatibility, and simple green preparation process, PDA has become a potential antibacterial material. The main antibacterial mechanism and pathway of PDA can be summarized into the following four parts: (1) contact-active antibacterial effect. PDA can destroy the structure of the bacterial cell membrane through the chelation of ions/proteins and the electrostatic effect.[42] (2) Good photothermal conversion ability. In the PDA system, the conjugated structure of indole-5,6-quinone and the electron donor–acceptor structures between 5,6-dihydroxyindole synergistically provides a wide range of light absorption.[43,44] (3) Generate reactive oxygen species (ROS). Due to a large amount of catechol in PDA, it can generate ROS through the transfer of electrons due to phenolic quinone isomerism and chelate ions *via* the catechol of PDA to destroy the bacterial cell wall.[39] (4) Direct chemical modification of PDA. Converting PDA to *N*-halamine by chlorination can also give PDA effective antibacterial properties *via* the destructive effect of halogen ions.[45] In this section, we will discuss the antibacterial mechanism of PDA itself as an antibacterial material and related works reported that are also summarized in Table 1 in detail.

### 2.1 Contact-active antibacterial effect

Generally, there are two main contact-active antimicrobial mechanisms (Fig. 1a). One is based on the catechol of PDA, which is similar to the antibacterial mechanism of some natural polyphenols such as tannic acid.[46] Specifically, catechol can chelate the metal ions for the need of normal physiological activities of bacteria as well as some special heteromeric proteins on the cell membrane, which disturb the normal physiological metabolism of bacteria; thus, the bacterial structure collapses.[47] Another antimicrobial mechanism that is speculated is that the antibacterial property of PDA may be caused by the protic amine groups since the contact of the positively charged functional groups with the cell wall of bacteria leads to the lysis of the bacteria and the exudation of cell contents. Although the total surface charge of membrane PDA is negative at pH > 4, protonated amines still exist in PDA. Amino dissociation has been proved to be qualitatively related to the bactericidal ability of PDA.[42] In 2012, Iqbal *et al.*[48] coated PDA on *E. coli* and found that it had over 99% inhibition effect. The PDA bacterial coating not only made it fully contact with the bacterial surface but

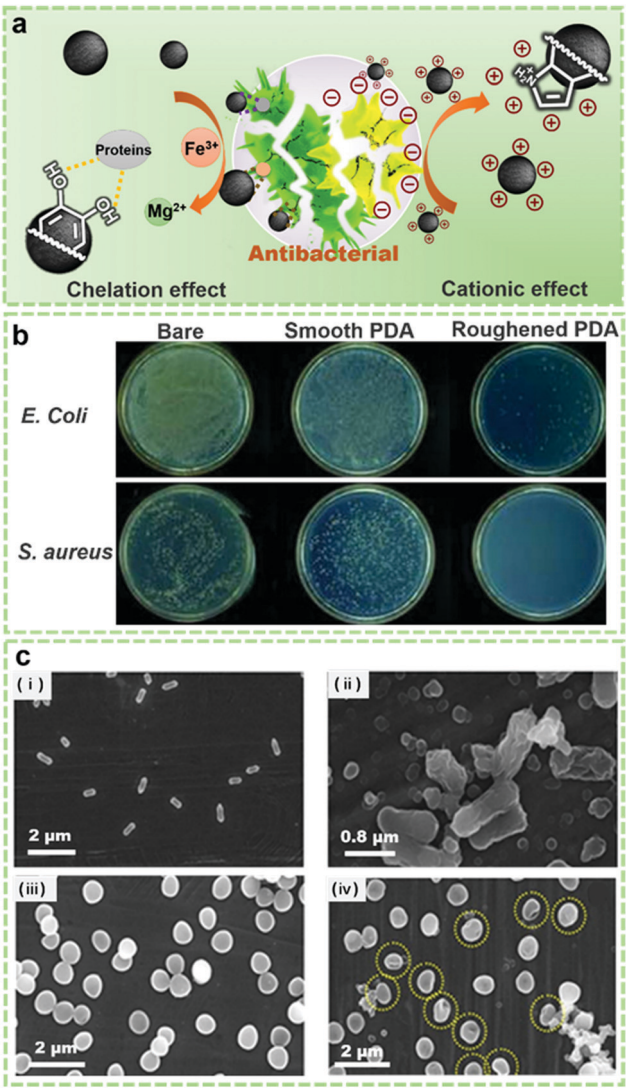


Fig. 1 (a) Schematic illustration of two main contact-active antimicrobial mechanisms of PDA: chelate action and cation-interaction. (d) Photographs of *E. coli* and *S. aureus* colonies on the agar plate after contact with the bare substrate, smooth PDA coatings, and roughened PDA coatings.[36] Copyright 2016, Springer Nature. (c) SEM images of *E. coli*/*S. aureus* before and after treatment with roughened PDA coating.[36] Copyright 2016, Springer Nature.

also controlled the bacterial division and hindered the normal metabolism.

However, the antibacterial ability of PDA is highly reliant on the material preparation method. As for the contact-active antibacterial effect, the contact area is significant. For instance, the bactericidal ability of the PDA-coated material can be related to the roughness of the coating. The self-polymerization of dopamine in a static solution can produce a relatively smooth PDA coating while a rough PDA coating can be obtained by adding a simple oscillation condition. Su *et al.*[36] reported that the roughened PDA coating showed enhanced contact activity against Gram-positive *S. aureus*, Gram-negative *E. coli*, and *P. aeruginosa* (Fig. 1b and c). The surface roughness of PDA would increase the surface irregularity, which is conducive for the landing and accumulation of free-swimming bacteria, thus increasing the capturing capability of PDA for bacteria and improving the sterilization efficiency.

### 2.2 Photothermal antibacterial effect

Near-infrared light, which has a wavelength of 700 to 1400 nanometers, penetrates the mammalian bodies with minimal damage to normal tissues. Photothermal materials have a strong ability to absorb near-infrared light and can convert light energy into heat. Common bacteria are thought to be sterilized at temperatures above 55 °C due to the denaturation of heat shock proteins. The generated heat can inhibit the development of drug-resistant bacteria and prevent the formation of biofilm structures. The mechanism of photothermal sterilization, on the one hand, can be explained as irreversible damage of the proteins or enzymes, which makes most of the physiological activities of microorganisms suffering damage. On the other hand, adequate heat can rupture the microbe's cell membrane, causing the cell contents to leak out. Therefore, as a new method of heating with high biocompatibility and medical efficiency, photothermal therapy (PTT) is considered as a safe and effective strategy to treat bacterial infections.[49] Numerous studies have proved that PDA has a high near-infrared absorbance and extraordinary photothermal conversion capacity and the obvious absorption of near-infrared wavelengths, which is thought to be the result of the subsequent self-polymerization of dopamine into dopaquinone and dopa-indole.[20] It has been reported that electron donor–acceptor structures can influence the light absorption property through the change in the bandgaps and 5,6-dihydroxyindole and indole-5,6-quinone in PDA can be regarded as a donor–acceptor structure.[43,44] At the same time, the conjugated structures of indole-5,6-quinone can also contribute to the broad-spectrum absorption of PDA. In general, PDA can take advantage of its excellent photothermal properties to participate in the construction of antibacterial materials in the form of photothermal auxiliaries (Fig. 2a). For example, Lei *et al.*[50] reported that a simple and effective ultrathin antimicrobial PDA coating with independent local microbe killing capacity was prepared. Also, the PDA coating could be further prepared on polymer medical catheters, which showed high photothermal sterilization efficiency. Besides, by combining with the fluorescence resonance energy transfer (FRET) assay and the photothermal capabilities of PDA, intelligent nanometer probes can be constructed with fluorescence imaging and antibacterial capabilities. Ye and his collaborators[38] realized this possibility. Through the prominent photothermal effect of PDA, it could effectively kill *S. aureus* biofilms, realizing the integration of the accurate identification of *S. aureus* drug-resistant biofilms and the function of efficient photothermal resistance biofilms (Fig. 2b). PDA NPs could be directly doped into the hydrogel as photothermal auxiliaries, in combination with the characteristics of the hydrogel itself to promote wound repairing and accelerating angiogenesis as a good antibacterial repair material. Han and his partners[37] used this strategy to prepare a chitosan/silk fibroin cryogel containing PDA NPs with high antioxidant capability and photothermally-assisted antibacterial capability.

 

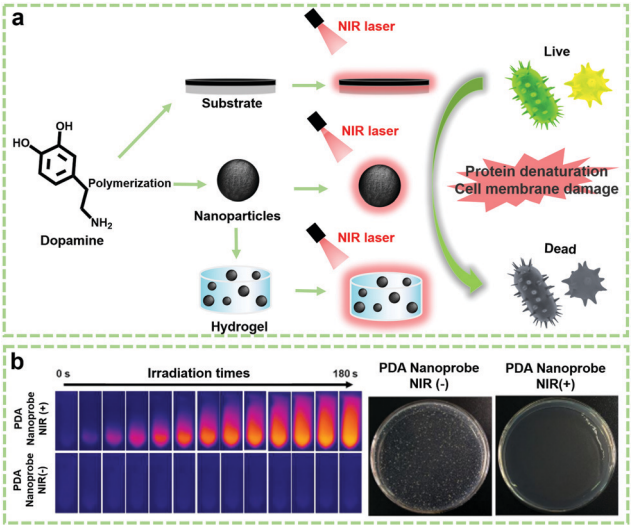


Fig. 2 (a) Schematic of photothermal antibacterial effects involving PDA. (b) Thermal images of PDA-based nanoprobe with or without NIR irradiation, and photographs of *S. aureus* colonies grown on LB agar plates.[38] Copyright 2020, American Chemical Society.

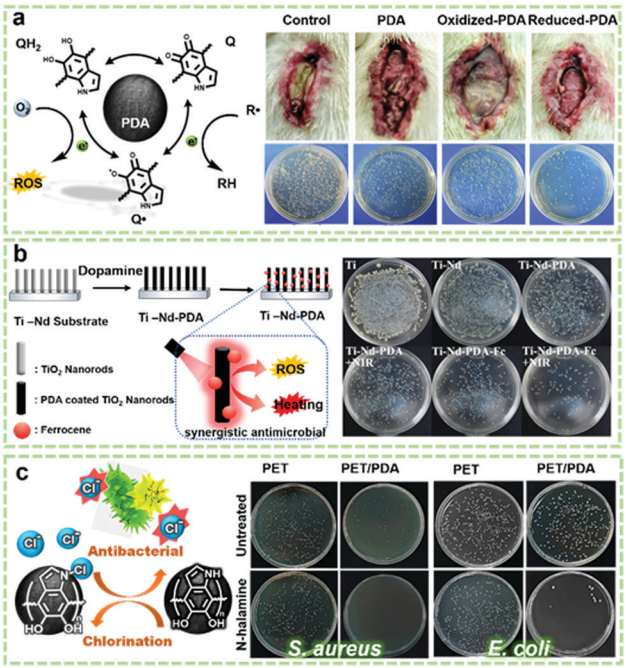


Fig. 3 (a) The redox state-dependent antibacterial property of PDA.[39] Copyright 2019, Elsevier. (b) The photodynamic antibacterial behavior of PDA-ferrocene coated $TiO_2$ nanorods.[53] Copyright 2020, American Chemical Society. (c) *N*-Halamine PDA showed an excellent antibacterial effect towards *S. aureus* and *E. coli*.[45] Copyright 2020, Elsevier.

Note that the photothermal ability of PDA can still be further improved. Our previous study has demonstrated that the metal ion-doped PDA materials enhanced the photothermal performances because of their narrower energy bandgaps.[51] Besides, we have also constructed donor–acceptor microstructures within PDA to enhance the NIR light absorption[40] since the existence of the donor–acceptor system can decrease the energy bandgaps and increase the electron delocalization, finally resulting in a significant increase in the photothermal effect.[39] With the enhancement of the photothermal effect, PDA antibacterial materials would perform with improved antibacterial ability, which broadens their applications.

### 2.3 ROS-production antibacterial effect

The production of ROS is a major biological method of sterilization. Compared with traditional sterilization methods, ROS therapy has higher efficacy and lower side effects. In early 2005, it was reported that melanin might be redox-active,[52] which could provide an additional active antibacterial mechanism by catalyzing the transfer of electrons from the endogenous extracellular region to $O_2$ to sustain ROS production. As an artificial melanin, PDA can both accept the electrons from the reducing agent and transfer them into the oxidizer. If the electron donor is a free radical, PDA will quench the free radical and show free radical scavenging ability; if the donor is oxygen, it will lead to the production of hydrogen peroxide free radicals. This process is thought to involve reducing catechol ($QH_2$), semiquinone free radicals ($Q^{\bullet}$), and oxidized *o*-quinone (Q) (Fig. 3a). Dr Qu *et al.* further confirmed this through electrochemical reverse engineering.[39] They found that the electron-donating ability of PDA depended on its redox state and was affected by the combination of metal ions and near-infrared irradiation. Thermal effects accelerated the kinetics during this process. The ROS produced by PDA may destroy the cell envelope of the bacteria and cause the substances in the cells to leak out, eventually causing the death of the bacteria. On this basis, they prepared PDA-ferrocene functionalized $TiO_2$ nanorods as implant materials with an antibacterial interface for preventing bacterial adhesion.[53] The $TiO_2$ nanorods surface was first prepared by the hydrothermal method to form a nanostructure to suppress the bacterial adhesion (Fig. 3b). Then, PDA was coated before modification *via* the covalent grafting of the iron-containing organometallic compound ferrocene. The PDA-treated ferrocene-functionalized $TiO_2$ nanorods (Ti-Nd-PDA-Fc) could offer photothermal effect and hydroxyl radical generation, providing an antibacterial efficacy of over 99% against methicillin-resistant *S. aureus* and *E. coli*. Besides, based on this strategy, our recent work proved that through the pre-treatment of PDA, the PDA-incorporated polysaccharide hydrogel showed evident antibacterial effect against *S. aureus*.[54]

### 2.4 *N*-Halamine antibacterial effect

*N*-Halamine is an emerging antibacterial technology, which has a broad spectrum of antibacterial effects on microorganisms, low toxicity to the human body, and good stability. *N*-Halamine usually contains the halogenated imide, amide, or amine group, which acts directly on the mercaptan or amino groups in the protein biological receptors, resulting in cell inhibition or inactivation.[55] Besides, *N*-halamines can be recharged after the rechlorination treatment.

There are many amino groups in the PDA system that make it an ideal precursor of antibacterial *N*-halamines. The amino groups on PDA can be chlorinated by exposure to a dilute

Table 2 Summary of antibacterial behaviors of PDA-based composite materials

| Major component | Antibacterial mechanism | Bacteria | Effect | Ref. |
|---|---|---|---|---|
| PDA/metal | $Ag^+$ release | *Bacillus acidicola* | Effective | 68 |
| PDA/metal | $Ag^+$ release | *E. coli* | ~97.9% | 70 |
| | | *S. aureus* | ~99.8% | |
| PDA/metal | $Ag^+$ release | *Vibrio parahaemolyticus strain 2A1* | Effective | 69 |
| | | *Enterococcus faecalis strain F1B1* | | |
| | | *Enterococcus faecalis strain FF11* | | |
| PDA/metal | $Ag^+$ release | *S. aureus* | 91.30% | 73 |
| PDA/metal | $Ag^+$ release | *E. coli* | 78% | 63 |
| | | *S. aureus* | 59.3% | |
| PDA/metal | $Ag^+$ release | *E. coli* | ~99% | 66 |
| | | *S. aureus* | | |
| | | MRSA | | |
| PDA/metal | $Ag^+$ release | *A. fumigatus* | Effective | 72 |
| | | *P. aeruginosa* | | |
| PDA/metal | $Ag^+$ release | *E. coli* | ~94.4% | 67 |
| | | *S. aureus* | ~1.8% | |
| PDA/metal | $Ag^+$ release | *E. coli* | Effective | 101 |
| | | *S. aureus* | | |
| PDA/metal | $Ag^+$ release | *E. coli* | 82% | 62 |
| | | *Bacillus* | 84% | |
| PDA/metal | $Ag^+$ release & PTT | *E. coli* | 99.99% | 65 |
| PDA/metal | $Ag^+$ release & PTT | *E. coli* | Effective | 71 |
| | | *S. aureus* | | |
| PDA/metal | PDT & PTT | *E. coli* | 96.8% | 75 |
| | | *S. aureus* | 95.2% | |
| PDA/metal | $Cu^{2+}$ release | *E. coli* | Effective | 86 |
| | | *S. aureus* | | |
| PDA/metal | $Cu^{2+}$ release | *S. aureus* | 99.9% | 84 |
| PDA/metal | $Cu^{2+}$ release | *E. coli* | ≥95% | 89 |
| | | *S. aureus* | | |
| | | *S. aureus* | | |
| | | *Kanamycin-resistant E. coli* | | |
| PDA/metal | $Cu^{2+}$ & $Ag^+$ release | *E. coli* | Effective | 85 |
| | | *S. aureus* | | |
| PDA/metal | Adhesion resistant | *E. coli* | 99.92% | 82 |
| PDA/drugs | NIR triggered antibiotics release | *S. aureus* | ~99.88% | 97 |
| PDA/drugs | PTT & NIR triggered antibiotics release | MRSA | ~100% | 100 |
| PDA/drugs | Antibiotics | *E. coli* | Effective | 58 |
| | | *S. mutans* | | |
| PDA/drugs | Antibiotics & $Ag^+$ release | *E. coli* | ~100% | 90 |
| | | *S. aureus* | | |
| PDA/drugs | Antibiotics & $Ag^+$ release | *E. coli* | >99.9% | 99 |
| PDA/drugs | Antibiotics release | *P. gingivalis* | >98% | 91 |
| | | *S. mutans* | ~92% | |
| PDA/drugs | Antibiotics release | *S. aureus* | Effective | 95 |
| | | MRSA | | |
| | | *P. aeruginosa* | | |
| PDA/drugs | Adhesion resistant | *E. coli* | Effective | 93 |
| | | *B. subtilis* | | |
| PDA/drugs | Blocked the growth of bacteria | *E. coli* | Effective | 96 |
| | | *S. aureus* | | |
| PDA/drugs | Damage cellular integrity | *A. acidoterrestris* | | 94 |
| PDA/drugs | Inherent antibacterial ability of ε-poly-l-lysine | *E. coli* | 95% | 92 |
| | | *S. aureus* | 100% | |
| PDA/drugs | Degrade the bacteria cell wall | *S. aureus* | Effective | 59 |
| PDA/carbon composite | $Ag^+$ release | *E. coli* | Effective | 102 |
| | | *P. aeruginosa* | | |
| | | *S. aureus* | | |
| | | *L. fusiformis* | | |
| PDA/carbon composite | PTT | *E. coli* | ~100% | 116 |
| | | *S. aureus* | | |
| PDA/carbon composite | PDT & PTT | *E. coli* | ~0.57% | 105 |
| | | *S. aureus* | ~7.55% | |
| PDA/carbon composite | $Ag^+$ release | *E. coli* | Effective | 104 |
| PDA/carbon composite | $Ag^+$ release | *E. coli* | 77.3% | 101 |
| | | *S. aureus* | 81.2% | |
| PDA/polycation | Cation-interaction | MRSA | Effective | 106 |
| | | *S. aureus* | | |
| PDA/polycation | Cation-interaction | *S. epidermidis* | 87% | 110 |

 

Table 2 (*continued*)

| Major component | Antibacterial mechanism | Bacteria | Effect | Ref. |
|---|---|---|---|---|
| | | *E. coli* | Effective | |
| PDA/polycation | Cation-interaction | *E. coli* | Effective | 107 |
| PDA/polycation | Cation-interaction | *E. coli* | 99.8% | 109 |
| PDA/polycation | Cation-interaction | *S. aureus* | 99.9% | 108 |
| PDA/NO | NO-release | *E. coli* | Effective | 111 |
| | | *P. aeruginosa* | | |
| PDA/NO | NO-release | *P. aeruginosa PAO1* | 99.9% | 115 |
| | | *P. aeruginosa PA37* | 97% | |
| | | *S. aureus* | 99% | |
| PDA/NO | PTT & NO-release | *E. coli* | Effective | 112 |
| | | *S. aureus* | | |
| PDA/NO | PTT & PDT & NO-release | *S. aureus* | 99.0% | 113 |



bleach solution (Fig. 3c). According to this, Chien's group[45] prepared an *N*-halamine PDA coating co-deposited with polyethyleneimine (PEI). Compared with the PDA coating without chlorination, the antibacterial efficiency of the PDA coating treated with chlorination was significantly improved. Meanwhile, it also showed higher antibacterial activity against broad-spectrum microorganisms with repeatable properties. This work demonstrated a new possibility of dopamine itself as an antibacterial material and PDA displays better antibacterial properties through halamine, and has great potential in the field of antibacterials.

# 3 PDA-based composite antibacterial materials

PDA is widely used in the interface chemical modification of antibacterial composites and functional materials because of its rich chemistry and unique photothermal, antioxidant, adhesion, and biocompatible capacities.[56] Therefore, more studies are often designed to combine PDA as an optimized material with other antibacterial agents in order to obtain better antibacterial ability. Metal ions, antibiotics, QAS, and other antibacterial substances can be easily connected to the PDA modified surface by physical adsorption or chemical bonding to achieve controlled release, reduced toxicity, and other effects. Metal ion fungicides such as $Cu^{2+}$ can be chelated by PDA *via* catechol groups and due to the redox activity of PDA, silver/gold ions chelated on the PDA surface can be reduced to silver/gold nanoparticles *in situ*.[57] Other metal ions such as $Fe^{3+}$ can be involved as a controlled release agent or cross-linking point. Antibacterial drugs such as amino acids, antibiotics, antimicrobial peptides, and lysozymes can be adsorbed onto the surface of PDA by electrostatic, π–π, cation–π, hydrogen bonding, and hydrophobic interactions.[58,59] Antibacterial substances such as QAS can also be chemically attached to PDA surfaces or copolymerized with PDA. Moreover, carbon nanomaterials such as GO and CNTs can be easily coated by PDA to obtain better dispersibility and biocompatibility. The summary of the antibacterial behavior of PDA-based composite materials is shown in Table 2 in detail.

## 3.1 PDA/metal antibacterial composites

Many metal ions have excellent antibacterial properties and can be used to build antibacterial composites with PDA *via* ion chelation. As is known, Ag NPs are a new generation of antibacterial nanomaterials due to their large surface area and size/shape-dependent physical and chemical properties, which are more effective than bulk Ag materials with broad-spectrum antibacterial capability. Ag NPs can directly react with the sulfur-containing protein, then cause structural changes or functional impacts on the cell membrane of the bacteria. However, it is impractical for Ag NPs to be used as an antibacterial material alone because the aggregation, the uncontrolled release of $Ag^{+}$, and the promotion of bacterial adhesion will influence the antibacterial effect.[60] To solve these problems, researchers have found that PDA-loaded Ag NPs can effectively improve the stability and antibacterial activity of Ag NPs. Specifically, PDA can be combined with the nanosilver precursor-$[Ag(NH_3)]^{2+}$ *in situ* to produce nanosilver particles. This process does not require other reducing agents (Fig. 4a).[61] Furthermore, the presence of PDA can prevent the Ag NPs from being directly exposed to oxygen, slow down the release of $Ag^{+}$, and avoid the aggregation of nanoparticles *via* catechol chelation. In addition, due to the fact that PDA can stick to almost any substrate, researchers can prepare density-controlled antibacterial interfaces of Ag NPs on various substrate surfaces, such as particles,[62] titanium metal,[63] stainless steel,[64,65] fibers/fabrics,[66] micro-nanofiltration membranes,[67,68] cellulose paper,[69] polymers,[70,71] and even contact lenses.[72] Besides the *in situ* preparation of Ag NPs on the PDA layer, there are many other well-designed methods for the preparation of PDA/Ag composite antibacterial materials.[73,74] These are because the surface of the PDA coating is rich in active catechols and amines, which are beneficial for the secondary reaction and the further modification of the surface. Similarly, gold nanoparticles (Au NPs) can also be loaded *in situ* on PDA surfaces. Combined with its catalytic ability, PDA-assisted Au nanomaterials can be fabricated *via* photodynamic/photothermal antibacterial synergy (Fig. 4b).[75]

$Cu^{2+}$ is an important component of biological proteins or enzymes. Compared to other antibacterial metals such as Ag/Au, $Cu^{2+}$ offers the best trade-off between the antibacterial effect and

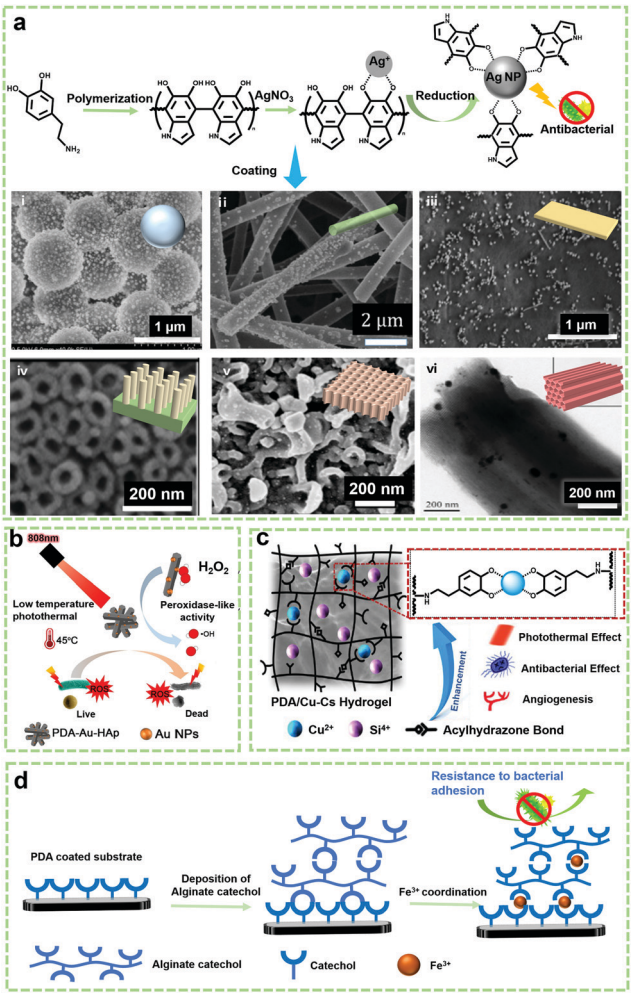


Fig. 4 (a) *In situ* fabrication of Ag–PDA composites on various surfaces and the related SEM images. Ag–PDA composites on: (i) nanoparticles.[76] Copyright 2014, Royal Society of Chemistry. (ii) Fibers.[77] Copyright 2015, American Chemical Society. (iii) Metal.[78] Copyright 2017, Elsevier. (iv) Nanorods.[79] Copyright 2015, Royal Society of Chemistry. (v) Filtration membranes.[67] Copyright 2016, American Chemical Society; (vi) mesoporous silica.[80] Copyright 2020, American Chemical Society. (b) Au nanoparticles loaded on the PDA surface with NIR response antibacterial effect.[75] Copyright 2018, Elsevier. (c) PDA/Cu hydrogel "hot-ion" antibacterial effect for skin-wound healing.[81] Copyright 2020, American Chemical Society. (d) PDA/$Fe^{3+}$ build multilayered anti-adhesion and antibacterial alginate films.[82] Copyright 2016, Wiley-VCH.

cytotoxicity with a low preparation cost. However, the sterilization of $Cu^{2+}$ requires a lengthy process and has certain toxicity at a high concentration.[83] Through the combination with PDA, the release of $Cu^{2+}$ can be controlled and a mild and long-acting antibacterial effect can be obtained (Fig. 4c). Inspired by this, Yeroslavsky and his coworkers[84] sonochemically produced PDA nanocapsules, which effectively chelated with $Cu^{2+}$, resulting in a selective antibacterial activity. In their follow-up work, nanosilver and $Cu^{2+}$ could be encapsulated in the capsule at the same time to achieve a better synergistic sterilization effect.[85] In addition, $Cu^{2+}$ also has the ability to promote bone repair and accelerate angiogenesis; thus, the PDA-assisted titanium alloy surface having $Cu^{2+}$ with sustained-release sterilization ability can be significant.[86] Wang and his coworkers also proved this point of view.[87] Also, PDA-assisted $Cu^{2+}$ antibacterial material can also be used for wound healing[81] and so on.[88,89] PDA can also be chelated with other metals to enhance their antibacterial effects from the structural design. Kim *et al.*[82] carried out the one-dimensional copolymerization of alginate with dopamine (Alg-C), which had good non-fouling property due to dense hydration layers formed by Alg (Fig. 4d). In an acidic environment, $Fe^{3+}$ was chelated with the catechol groups of PDA to make cross-linking Alg-C, and finally multi-layer alginate films with excellent antibacterial ability were obtained. Therefore, PDA could not only play a role in the stabilizing metal ions by catechol chelation but also provides functions to enhance the antibacterial properties of the PDA/metal antibacterial composites.

### 3.2 PDA/antibacterial drug composites

Antibacterial drugs including antibiotics, antibacterial peptides, and lysozymes can be physically or chemically connected with PDA (Fig. 5). Antibiotics are one of the most widely used antibacterial drugs but their abuse has led to an increase in the bacterial resistance and the biotoxicity of some antibiotics is also not negligible. Therefore, to make more efficient and safer usage of antibiotics, researchers have connected antibiotics with other components utilizing physical cross-linking or chemical connection to achieve long-term and on-demand drug release. Likewise, PDA can be chosen as an anchor for antibiotics to fabricate antibacterial materials with long-circulation (Fig. 6a). For instance, Ma *et al.*[90] developed a chemo-Ag nanohybrid compact therapeutic based on vancomycin-encapsulated the PDA–Ag NPs nanohybrid. Vancomycin was loaded on PDA NPs through π–π stacking electrostatic interactions and hydrogen bonding. In addition, the chemical structure of PDA also allowed

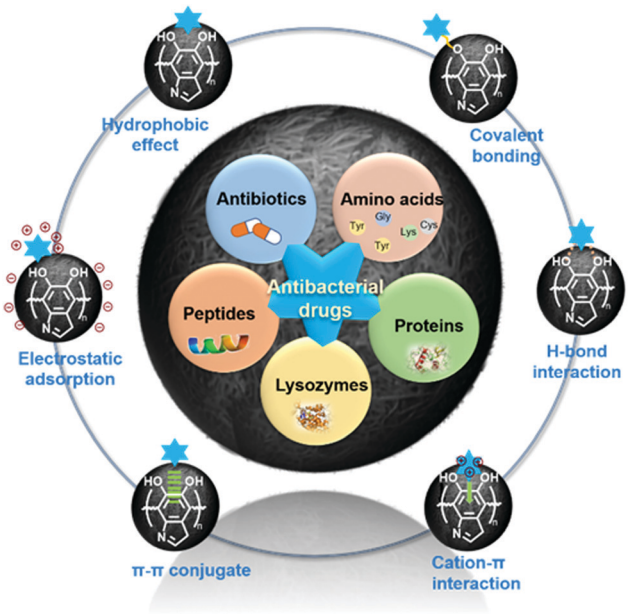


Fig. 5 Schematic of the PDA/antibacterial drug composites.

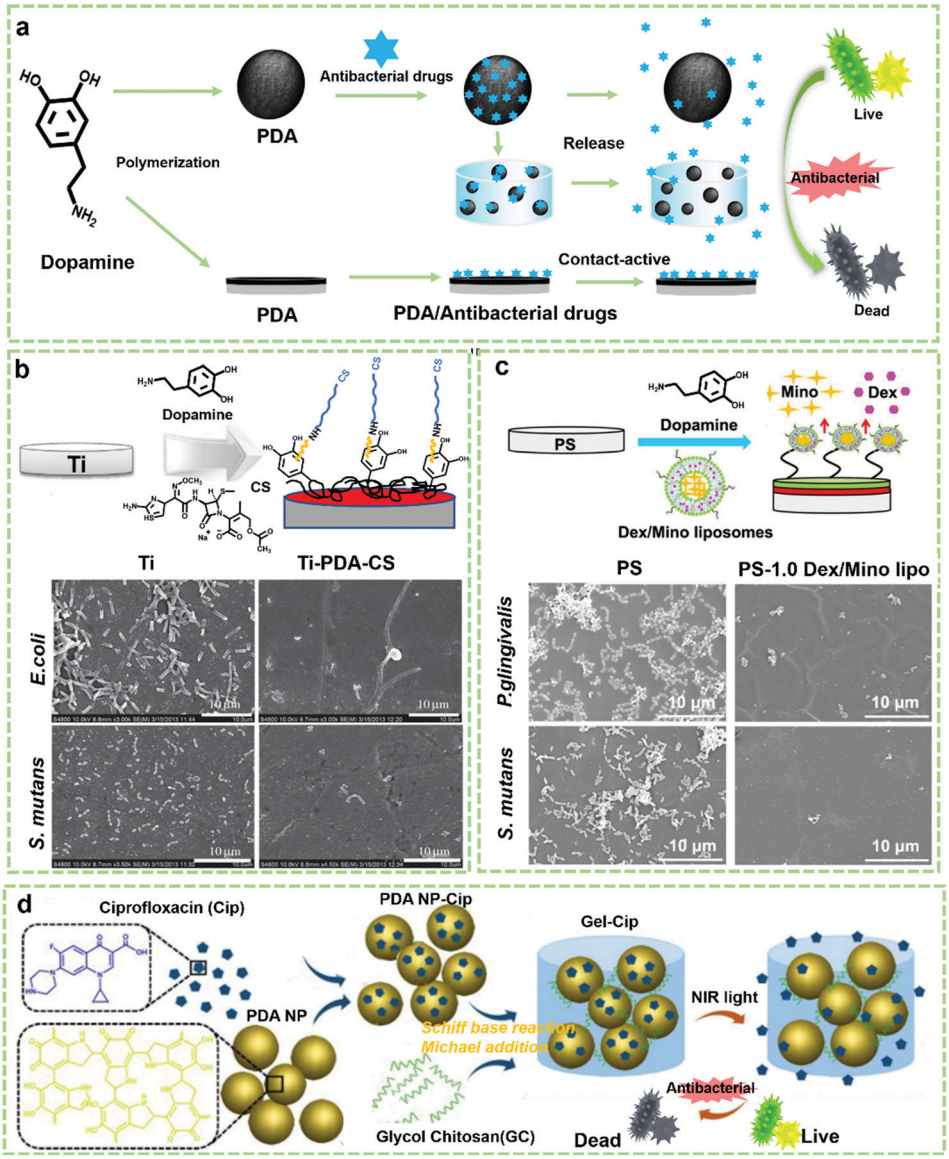


Fig. 6 (a) Schematic illustration of the fabrication of the PDA/antibacterial drug composite materials. (b) The PDA/Ti/cefotaxime sodium (CS) composite exhibited antibacterial performance against *E. coli* and *S. mutans*, and the related SEM images.[58] Copyright 2014, Royal Society. (c) The PDA/dexamethasone (Dex)/minocycline (Mino)-loaded liposomes antibacterial surface exhibited antibacterial performance against *E. coli* and *S. mutans*, and the related SEM images.[91] Copyright 2017, American Chemical Society. (d) PDA/ciprofloxacin contained hydrogel with NIR-triggered on-demand antibiotic releasing antibacterial property.[97] Copyright 2019, Elsevier.

various antibiotics containing amino and sulfhydryl groups to be firmly attached to the surface by the Schiff base and Michael addition. Through this covalent bonding, He *et al.*[58] coated PDA on Ti and then cefotaxime sodium was loaded chemically (Fig. 6b). Xu's group[91] also prepared PDA/dexamethasone plus minocycline-loaded liposomes antibacterial surfaces on polystyrene (Fig. 6c). These kind of modified Ti substrates with enhanced antibacterial activity could hold great potential as implant materials for applications in dental and bone graft substitutes.

Other biological antibacterial drugs, such as amino acids, antimicrobial peptides, proteins and lysozymes, and modified antimicrobial surfaces combined with PDA have also been widely reported. They can also be decorated on PDA non-covalently or covalently to get a better synergistic antibacterial effect. For example, some amino acids have high antifouling and antibacterial properties such as lysine. By simulating the natural mussel foot protein mfp-5, hydrogels containing PDA and polylysine with high adhesion and high antibacterial ability were prepared.[92] On the wet tissue surface, the hydrogel showed outstanding adhesion property and inherent antibacterial property due to the cooperation effect of catechol-Lys. α-Aminoisobutyric acid,[93] nisin,[94] branched antimicrobial peptide (B4010),[95] lactoferrin,[96] and lysostaphin[59] have also been reported for building highly effective antibacterial surfaces by PDA-assisted strategy.

Through physical cross-linking or chemical connection, antibacterial surface treatment can be incorporated with antibacterial

efficiency for a long period of time and is less liable to produce resistant strains. Meanwhile, it could be easy to offer an on-demand release profile of the antibacterial drugs. Through near-infrared photothermal action, the drugs physically adsorbed on PDA can be release in a controlled manner, leading to a synergistic therapy action.[98] Combined with the photothermal property, PDA antibacterial materials can achieve photothermal sterilization and infrared controlled drug release synergistic effect. Recently, Ran *et al.*[99] loaded colistin on PDA NPs *via* electrostatic and hydrophobic interactions as well as covalent bonding and were decorated with Ag NPs. Also, the colistin and Ag NPs could be released persistently *via* in a near-infrared laser-triggered manner. He *et al.*[100] reported a highly effective chemothermal treatment platform based on PDA-coated gold nanorods. Specifically, the PDA-coated gold nanorods were grafted with glycol chitosan and were loaded with daptomycin. It possessed pH-sensitive and photo-thermal triggered daptomycin release ability. Gao *et al.*[97] fabricated an injectable hydrogel by mixing ciprofloxacin-loaded PDA NPs *via* the π–π stacking and/or hydrogen bonding interactions with glycol chitosan. Ciprofloxacin could be released under NIR irradiation trigger (Fig. 6d). The main roles of PDA in PDA/antibacterial drug composites include improving the drug loading, enhancing the circulation time, and facilitating on-demand drug release.

### 3.3 PDA/carbon composite antibacterial materials

Carbon nanomaterials (CNMs) are among the most broadly discussed, researched, and applied synthetic nanomaterials including zero-dimensional carbon points, one-dimensional CNTs, and two-dimensional materials such as graphene. CNMs have high antibacterial activity due to their unique physico-chemical property and structural characteristics.[10] The sharp edges of some CNMs can cause physical damage on direct contact with the bacterial membrane. Besides, the photothermal effect and packaging effect of CNMs are also related to the mechanism of physical damage. The chemical action is related to the charge transfer and oxidative stress generated by the generated ROS. However, the potential toxicity of CNMs is barely discussed. Also, surface inertia, easy aggregation, and poor biocompatibility still limit their wider application in the field of antimicrobial resistance, while PDA can modify the surface of the carbon material through its unique characteristics of adhesion *via* hierarchical interactions, biocompatibility improvement, and CNMs dispersibility. Moreover, PDA could also provide many chemically active sites for secondary modification to build composite antibacterial materials with better antibacterial effect.

Generally, PDA can be introduced into carbon composite antibacterial materials in two ways (Fig. 7a). One is to obtain a PDA-containing polymer firstly, which was prepared through chemical modification, and then it could be decorated on the CNMs physically. Nie and coworkers[101] fabricated mussel-inspired Ag–carbon nanotube composites with good sterilization effect through this method and the PDA-conjugated polymer coatings offered better biocompatibility. Similarly, Khamrai's group[102] also employed this strategy. In addition, Liang *et al.*[103] prepared an

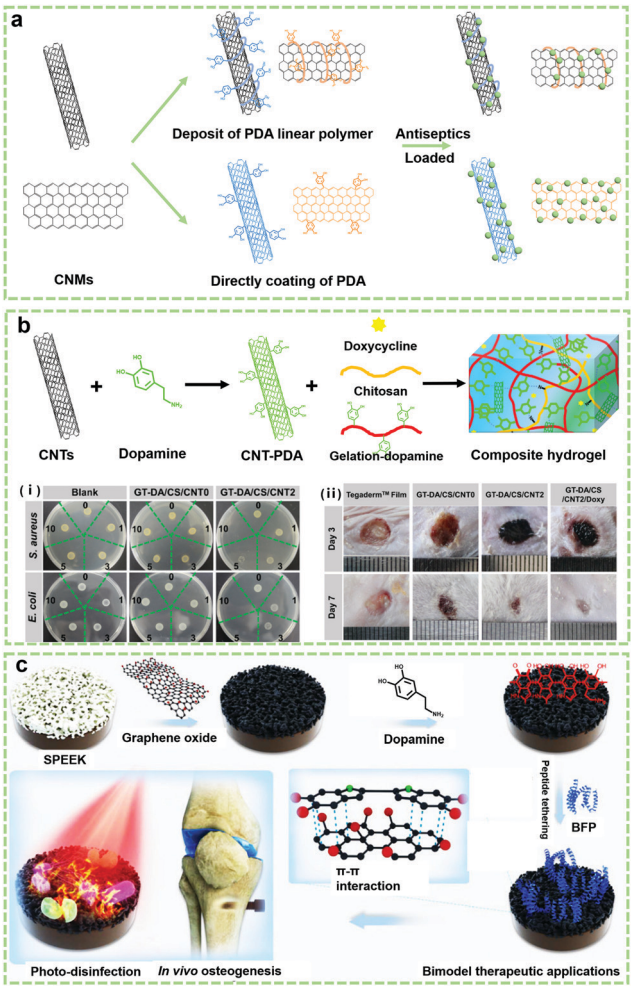


Fig. 7 (a) Schematic of the two ways towards PDA-assisted CNMs antibacterial composites. (b) Fabrication, antibacterial, and wound healing performance of PDA-coated CNTs-based composite hydrogels.[103] Copyright 2019, Elsevier. (c) GO/PDA/oligopeptide decorated sulfonated polyetheretherketone (SPEEK) implant has photo-disinfection and osteogenic ability.[105] Copyright 2020, Royal Society of Chemistry.

injectable composite hydrogel with antibacterial conductivity and antioxidant activity. Dopamine was first grafted on gelation, then CNTs coated with chitosan and PDA were used to build the GT-DA/CS/CNT composite hydrogels. PDA here provided excellent adhesion and improved the dispersion of the CNTs (Fig. 7b).

Besides, the direct coating of PDA on CNMs is also an effective strategy of material construction. With the introduction of PDA, CNMs can be combined with the Ag NPs and other antimicrobial agents, which can easily achieve a better synergistic antibacterial effect, better biocompatibility, as well as long-term stability. In 2012, Zhang *et al.*[104] prepared Ag/PDA/GO nanosheets for the first time. It was regarded as a great potential antibacterial material with green and environment-friendly preparation methods. Meanwhile, the loading of other functional materials can bring additional effects. For example, Wang *et al.*[105] assembled GO, PDA, and osteogenic oligopeptide onto the surface of porous sulfonated PEEK. The composite coating films had synergetic photothermal/photodynamic therapeutic effects and

 

promoted *in vivo* osseointegration and bone remodeling significantly (Fig. 7c).

### 3.4 PDA/polycation composite antibacterial materials

Through electrostatic force, hydrogen bonding force, and hydrophobic binding force between the protein molecules and positively charged QAS, QAS is adsorbed on the negatively charged wall of the bacteria in order to change the permeability of the wall and break the bacterial structure. However, it has a short-term antibacterial ability and the abuse of QAS can cause environmental toxicity.[7] Polymerization into macromolecules can solve the above problems largely due to the prolonged antibacterial effect, good chemical stability, impermeability to the skin, and reduced environmental toxicity; however, the poor cell and tissue affinities limit their applications in the biomedical field. The abundant chemistry of PDA provides a large number of reaction sites, which can be easily connected with QAS through copolymerization, chemical modification, or physical absorption, and the involvement of PDA can bring better biocompatibility, adhesiveness, and surface modification capability (Fig. 8).

For the direct chemical modification of the PDA coating, Ding *et al.*[106] firstly synthesized thiol-terminated diblock copolymers of PEG and cationic polycarbonates (HS-PEG–PCN) with various compositions through the Michael addition reaction. The polymer was then grafted onto the PDA-coated surface to form an antibacterial and antifouling interface material. Other researchers have followed this strategy. For example, Jin and coworkers[107] conjugated bromoalkyl initiators to PET sheets coated with PDA, and then *in situ* polymerized polycarboxybetaine and polysulfobetaine using ATRP reactions. Finally, the cooperative antifouling and antibacterial surface of the amphoteric polymer were formed on the surface of the PET sheet, which showed good blood compatibility. In addition, QAS polymers such as polyhexamethylene biguanidine (PHMB) can be conjugated on the PDA coating *via* cation–π interaction. Shi *et al.*[108] indicated this point and fabricated a PHMB/PDA bio-interface with superior antibacterial and osteoinductive capability. Dopamine could be connected to QAS through one-dimensional copolymerization, and injectable self-healing hydrogels based on catechol-mediated hydrogen bond and aromatic interactions could be obtained. For example, Li's group[109] synthesized a tri-block copolymer contained catechol and QAS. Through the self-assembly of the copolymer, an injectable self-healing hydrogel with antimicrobial and antifouling properties was obtained. Besides, Gan's group[110] prepared an antibacterial hydrogel by combining quaternized chitosan with dopamine methacrylamide and the 2-(dimethylamino)ethyl methacrylate copolymer. The hydrogel not only had excellent contact sterilization ability but also good toughness and adhesion. In the PDA/polycation composite materials, PDA mainly promotes the biocompatibility, interfacial affinity, and adhesive ability of the whole antibacterial materials.

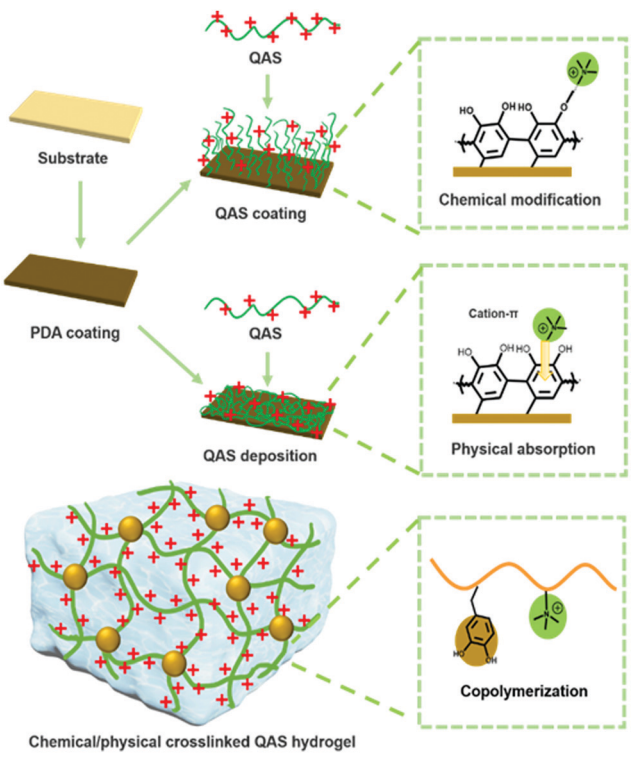


Fig. 8 Preparation of PDA/QAS antibacterial materials.

### 3.5 PDA/NO composite antibacterial materials

Endogenous gases such as nitric oxide (NO) and carbon monoxide (CO) have been widely investigated as antibacterial agents. NO radical (NO•) and its byproducts exhibit antibacterial effects on various kinds of bacterial species by inducing oxidative stress or nitrosative stress such as lipid peroxidation and DNA deamination.[112] There are many NO donors that can be modified in NO delivery systems such as *S*-nitrosothiol (RSNO), nitroglycerin, and *N*-diazeniumdiolate. Among them, *N*-diazeniumdiolate can be easily conjugated to secondary amine groups. Compared to other polyamines such as polyethyleneimines, PDA is a better material possessing good biocompatibility and low biotoxicity, and can be modified on various implant surfaces (Fig. 9a). Lee's group[114] first indicated the feasibility of NO-loaded PDA material through diazeniumdiolization in 2013. Then, in 2016, Park *et al.*[111] prepared diazeniumdiolate-functionalized PDA hollow nanoparticles. The PDA hollow nanoparticles were obtained by the silicon nanoparticle template-mediated process and then exposed to a high pressure of NO. The release of NO in the materials was also further explored and the antibacterial effect to Gram-negative bacteria including *E. coli* and *P. aeruginosa* was proved (Fig. 9b). Meanwhile, the antibacterial interface with the NO-releasing capability was reported;[115] Sadrearhami's group reported an antibiofilm NO-releasing PDA coating on a glass substrate with poly(ethylene glycol) connected *via* Michael addition. The coating released NO over 48 h and inhibited or killed the bacteria effectively (Fig. 9c). Due to the photothermal effect of PDA, the diazeniumdiolate-functionalized PDA material can obtain the ability of photothermal and photodynamic synergetic sterilization. Yu *et al.*[112] reported that they loaded NO onto the surface of the PDA-coated iron oxide nanocomposite, grafted by first three

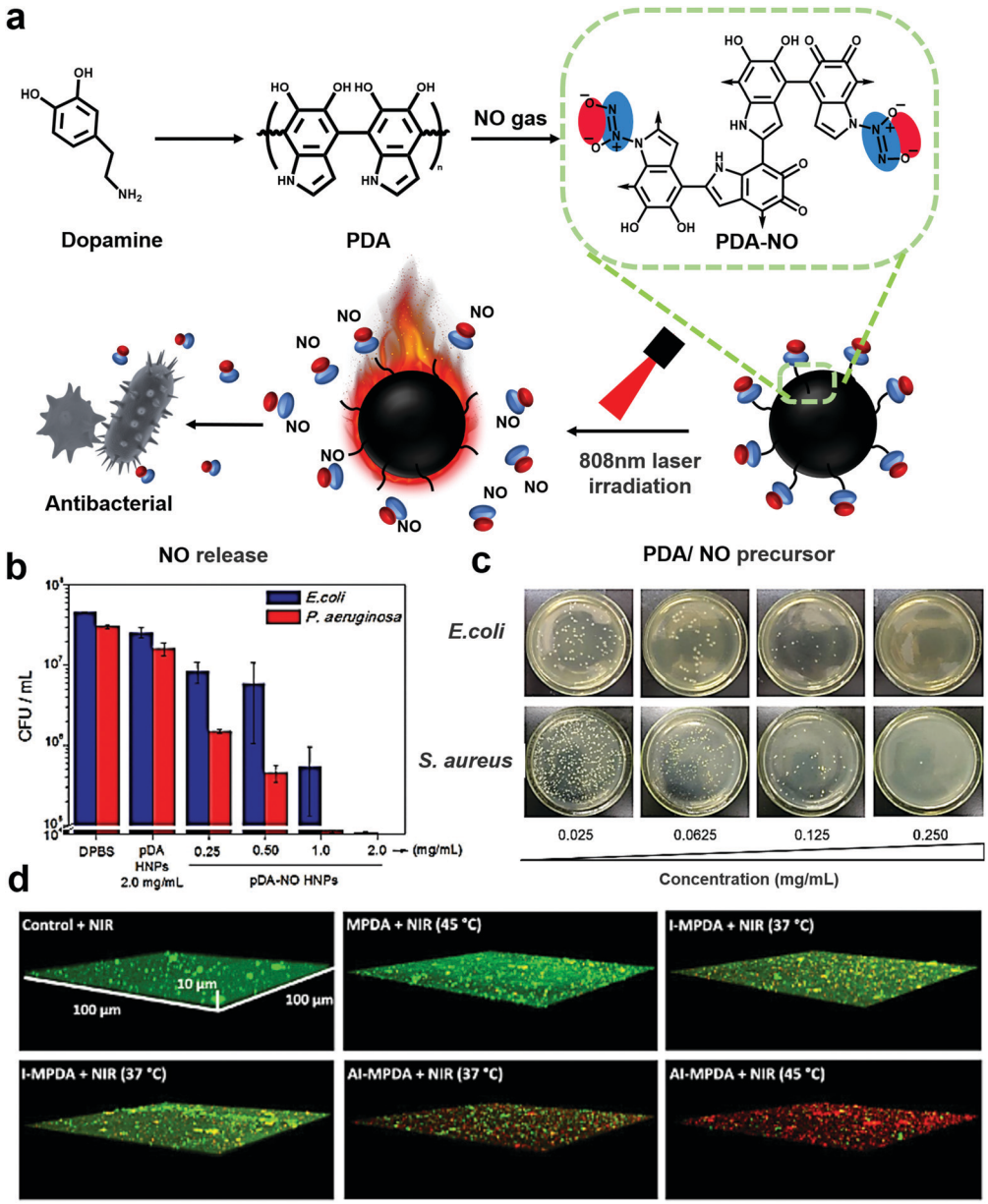


Fig. 9 (a) Schematic of the preparation and antibacterial mechanism of diazeniumdiolate-functionalized PDA triggered by NIR light. (b) Antibacterial activities of PDA–NO hollow nanoparticles on *E. coli* and *P. aeruginosa*.[111] Copyright 2016, Wiley-VCH. (c) Bacterial colony formation of *E. coli* and *S. aureus* treated with different concentrations of $Fe_3O_4$@PDA@PAMPAM@*N*-diazeniumdiolate.[112] Copyright 2018, Wiley-VCH. (d) 3D confocal laser scanning microscope (CLSM) of the live/dead bacterial staining results with different treatments.[113] Copyright 2020, American Chemical Society.

generated dendritic poly(amidoamine). The nanocomposite displayed controllable NO release property triggered by 808 nm laser irradiation, leading to an excellent synergistic antibacterial effect. In addition to *N*-diazeniumdiolate, other NO precursors such as L-arginine could also be introduced into the PDA systems. Yuan *et al.*[113] designed an antibacterial nanoplatform consisting of L-arginine, indocyanine green, and mesoporous PDA. After NIR irradiation, indocyanine green produced ROS based on the temperature increase, while L-arginine could produce NO gas under catalysis, leading to an excellent antibacterial effect (Fig. 9d). In this system, PDA could maintain the high loading of NO in the system with on-demand gas release profile. Besides, the photo-thermal effect of PDA could also enhance the antibacterial properties of the PDA/NO composite materials.

## 4 Reflections

So far, many kinds of PDA antibacterial materials and the corresponding antibacterial mechanisms have been investigated and established, including the antibacterial performances of free-standing PDA and PDA-based composite materials. It can be concluded that PDA plays a critical role in both types of antibacterial materials.

 

For free-standing PDA antibacterial materials, PDA can easily construct materials in various dimensions structurally for antibacterial applications, including dots,[33] surface coatings,[116] and nanoparticles.[117,118] Moreover, PDA has certain antibacterial functions due to its unique physical and chemical properties such as contact-active antibacterial, photothermal antibacterial, ROS induced antibacterial, and haloamine antibacterial effect. The contact-active antibacterial effect is mainly based on the abundant catechol groups and partial positive charges on the PDA surface.[119] The contact-active antibacterial effect is mainly influenced by the contact area. Usually, the rough surface coatings can contact the bacteria to a greater extent than the smooth surface coatings.[36] That is to say, the particle size and the morphology of PDA also have a certain impact on the total antibacterial effect due to the difference in the specific surface area. However, since the contact antibacterial only works on the interface, the sterilization effect on the large-dose bacterial environment is limited. The photothermal antibacterial ability of PDA is one of the most popularly used antibacterial strategies.[120] The excellent photothermal conversion ability of PDA allows the efficient conversion of infrared light into heat, which can play a role in high-temperature sterilization.[121] For *in vitro* antibacterial applications, the higher the photothermal conversion efficiency, the better the sterilization effect. However, for *in vivo* antibacterial applications, high-temperature conditions might also cause certain possible damages to normal cells and tissues. Therefore, it is necessary to balance the temperature damage and antibacterial behavior by controlling the temperature within a certain range to achieve a non-toxic and long-term sterilization effect.[37] Through further exploration and modification of the structure of PDA, more antibacterial methods can be explored. In recent years, it has been discovered that PDA possesses the capability of ROS-induced antibacterial and haloamination antibacterial effect. The mechanism of ROS-induced antibacterial effect mainly lies in the redox property of the multiple catechol structures, which enables the rapid acceptance and donation of electrons by PDA, furthering generating ROS in oxygen-rich environments.[39] This process can be dynamically accelerated under the irradiation of NIR light. Similarly, the secondary amine structure of PDA can be replaced by halogen atoms through the chemical reaction of haloamination.[55] Under certain conditions, halide ions could be released to show the antibacterial effects.[122] Notably, whether the material can maintain the antibacterial ability under complex conditions, whether it is selective for the type of bacteria, and the influencing factors of the chemical reaction need further research. However, as a potential antibacterial agent, free-standing PDA antibacterial materials have some advantages compared with the current mature antibacterial systems. For instance, compared with precious metal antibacterial agents such as Au and Ag, PDA has a lower preparation cost. Also, for commonly used antibiotics, PDA is less likely to cause bacterial resistance and has lower biological toxicity. Compared with antibacterial agents (such as QAS) that have a complex synthesis process, PDA is simple to prepare and is flexible, which can be easily and quickly coated on the surface of various devices.

In addition, due to the inherently promising chemical and physical features of PDA, this class of bioinspired materials can also serve as template materials to be incorporated with other kinds of antibacterial materials in order to further develop highly efficient antibacterial composite materials. The role of PDA in these functional composite materials could be mainly divided into structural and functional contributions, which make these PDA antibacterial composite materials multifunctional.

(a) Structural contribution. PDA is an important structural element in the construction of various functional composite materials. It has universal surface modification capabilities and can be used to construct multi-dimensional materials including two-dimensional surface coatings, three-dimensional nanoparticles, and hydrogels.[118] Then, it can be incorporated into other antibacterial agents *via* covalent linkages and non-covalent interactions, which are mainly due to the rich surface chemistry of PDA.[123] The rapid oxidative polymerization of catechol groups also enables PDA to construct the interfaces conveniently and quickly on various materials, and then covalently connect them through Michael addition and Schiff base reactions or metal chelate to load other antibacterial drugs, or adsorb antibacterial agents through hydrogen bonding, electrostatic adsorption, π–π interaction, or cation–π effect non-covalently.[124] Meanwhile, under some specific conditions, the antibacterial agents could exhibit stimuli-responsive behaviors and on-demand release profiles.[125] For example, nanodot antibacterial materials loaded with colistin and silver were prepared by Ran *et al.*[99] The binding of colistin was mainly through the electrostatic and hydrophobic interactions and the covalent connection, while nanosilver was further obtained *via* the reduction of chelating $Ag^{+}$. They proved that colistin and silver particles have different release profiles under different acidic environments and infrared light. This significantly improved the long-term antibacterial effect and reduced the biological toxicity of the antibacterial materials.

(b) Functional contribution. Note that some promising properties of PDA itself could also be involved in PDA-based antibacterial composite systems, including photothermal properties, biocompatibility, oxidation resistance, and adhesion properties.[19] Among them, the introduction of photothermal properties into PDA-based materials offers photothermal and photodynamic synergistic antibacterial effects. PDA provides high-temperature sterilization under infrared light radiation, and the antibacterial agents located on PDA can be released and show further antibacterial effect. Moreover, the mussel-inspired PDA hydrogel materials usually have excellent bioadhesive properties due to the presence of multiple catechol groups within PDA.[126] Besides, the anti-oxidation properties of PDA may also bring better radical scavenging effects to the whole composite materials.[127] Liang *et al.*[97] made the full use of these properties of PDA for composite material construction. The CNTs loaded in the gel showed better photothermal effect, dispersibility, and biocompatibility after being coated with PDA. After the coating, it exhibited better photothermal effect, dispersibility, and biocompatibility.

The current works on PDA antibacterial materials pay more attention to the anchoring effect of PDA as a structural element in composite materials and the synergistic sterilization effect of the photothermal function. Indeed, the improvement of the inherent antibacterial ability of PDA and PDA composite materials

mainly relies on the structural tailoring of PDA, including the surface density of the catechol groups, the presence of less compact π-stacked microstructures, and multiple donor–acceptor pairs within PDA. Also, with the further exploration and disclosure of the physical and chemical structure of PDA in the future, more PDA-based antibacterial materials with better antibacterial properties can be designed and developed.

## 5 Conclusion and perspective

This review mainly summarizes and discusses the current progress and further perspective of PDA-based antibacterial materials. In recent years, PDA has gradually emerged as a new substance in the field of antimicrobial resistance. Based on the photothermal effects, redox properties, and abundant chemicals including catechol and primary amino groups, the mechanism of its inherent antibacterial properties is also discussed. Due to its rich surface chemical properties, PDA composite antibacterial materials have strong advantages, including the efficient and convenient preparation of the PDA composite antibacterial interface. Common antibacterial substances such as Ag NPs, $Cu^{2+}$, antibiotics, CNMs, QAS, and NO gas can be combined with PDA by chemical coupling or physical adsorption. The PDA composite antibacterial material can realize the controlled release of antibacterial substances with efficient antibacterial ability and good biocompatibility after precise design. This makes PDA one of the most promising materials in the field of antimicrobial *in vivo* and implant interfaces.

Despite PDA-based antibacterial materials being widely explored, there are still some challenges that need to be conquered. Firstly, the antibacterial ability of PDA is relatively mild and cannot meet the higher antibacterial requirements. Other antibacterial substances are still needed to be introduced in order to achieve higher efficiency of sterilization. Hence, the improvement of PDA's inherent antibacterial properties is regarded as another interesting direction. The detailed understanding of the PDA polymerization mechanism is still controversial, and the in-depth exploration of its internal structure and polymerization mode is conducive for the further optimization of PDA functional modification. For instance, through the adjustment of the morphology or the microstructure of PDA, the contact-active and photothermal antibacterial efficiency can be significantly improved.[43] Besides, several chemical reactions such as halide ammonification of PDA or reverse-reduction to the state of PDA were also able to achieve a more efficient antibacterial effect.[39,45] PDA, as an important structural and functional building block for antibacterial composite materials, has both great fundamental and clinical value in the future.

## Conflicts of interest

The authors declare no conflict of interest.

## Acknowledgements

This work was supported by National Natural Science Foundation of China (21774079 and 21975167), the National Key R&D Program of China, Synthetic Biology Research (2019YFA0904500), the Program of the Science & Technology Department of Guangzhou, China (201803020039), and the Fundamental Research Funds for Central Universities.

## References

1 J. W. Costerton, P. S. Stewart and E. P. Greenberg, *Science*, 1999, **284**, 1318–1322.
2 Y. Huang and H. Huang, *Rare Met.*, 2019, **38**, 512–519.
3 C. R. Arciola, D. Campoccia and L. Montanaro, *Nat. Rev. Microbiol.*, 2018, **16**, 397–409.
4 Y. Wang, Y. Yang, Y. Shi, H. Song and C. Yu, *Adv. Mater.*, 2020, **32**, 1904106.
5 M. Li, H. Wang, J. Hu, J. Hu, S. Zhang, Z. Yang, Y. Li and Y. Cheng, *Chem. Mater.*, 2019, **31**, 7678–7685.
6 N. D. Stebbins, M. A. Ouimet and K. E. Uhrich, *Adv. Drug Delivery Rev.*, 2014, **78**, 77–87.
7 E.-R. Kenawy, S. D. Worley and R. Broughton, *Biomacromolecules*, 2007, **8**, 1359–1384.
8 A. Sirelkhatim, S. Mahmud, A. Seeni, N. H. M. Kaus, L. C. Ann, S. K. M. Bakhori, H. Hasan and D. Mohamad, *Nano-Micro Lett.*, 2015, **7**, 219–242.
9 S. Chernousova and M. Epple, *Angew. Chem., Int. Ed.*, 2013, **52**, 1636–1653.
10 Q. Xin, H. Shah, A. Nawaz, W. Xie, M. Z. Akram, A. Batool, L. Tian, S. U. Jan, R. Boddula, B. Guo, Q. Liu and J. Gong, *Adv. Mater.*, 2019, **31**, 1804838.
11 H. Lee, S. M. Dellatore, W. M. Miller and P. B. Messersmith, *Science*, 2007, **318**, 426–430.
12 Y. Wang, Q. Huang, X. He, H. Chen, Y. Zou, Y. Li, K. Lin, X. Cai, J. Xiao, Q. Zhang and Y. Cheng, *Biomaterials*, 2018, **183**, 10–19.
13 F. Zhang, Q. Zhang, X. Li, N. Huang, X. Zhao and Z. Yang, *Biomaterials*, 2019, **194**, 117–129.
14 J. Bai, H. Wang, H. Chen, G. Ge, M. Wang, A. Gao, L. Tong, Y. Xu, H. Yang, G. Pan, P. K. Chu and D. Geng, *Biomaterials*, 2020, **255**, 120197.
15 X. Li, J. Liu, T. Yang, H. Qiu, L. Lu, Q. Tu, K. Xiong, N. Huang and Z. Yang, *Biomaterials*, 2020, **241**, 119904.
16 Z. Wang, Y. Zou, Y. Li and Y. Cheng, *Small*, 2020, **16**, e1907042.
17 Z. Li, T. Wang, F. Zhu, Z. Wang and Y. Li, *Chin. Chem. Lett.*, 2020, **31**, 783–786.
18 Y. Zou, T. Wu, N. Li, X. Guo and Y. Li, *Polymer*, 2020, **186**, 122042.
19 X. Zeng, M. Luo, G. Liu, X. Wang, W. Tao, Y. Lin, X. Ji, L. Nie and L. Mei, *Adv. Sci.*, 2018, **5**, 1800510.
20 Y. Liu, K. Ai and L. Lu, *Chem. Rev.*, 2014, **114**, 5057–5115.
21 P. Yang, Z. Gu, F. Zhu and Y. Li, *CCS Chem.*, 2020, **2**, 128–138.
22 S. Huang, N. Liang, Y. Hu, X. Zhou and N. Abidi, *BioMed Res. Int.*, 2016, **2016**, 2389895.
23 M. Liu, G. Zeng, K. Wang, Q. Wan, L. Tao, X. Zhang and Y. Wei, *Nanoscale*, 2016, **8**, 16819–16840.

 

24 J. Hu, L. Yang, P. Yang, S. Jiang, X. Liu and Y. Li, *Biomater. Sci.*, 2020, **8**, 4940–4950.
25 X. Cheng, M. Li, H. Wang and Y. Cheng, *Chin. Chem. Lett.*, 2020, **31**, 869–874.
26 H. Geng, L. Zhuang, M. Li, H. Liu, F. Caruso, J. Hao and J. Cui, *ACS Appl. Mater. Interfaces*, 2020, **12**, 29826–29834.
27 W. Shen, R. Wang, Q. Fan, X. Gao, H. Wang, Y. Shen, Y. Li and Y. Cheng, *CCS Chem.*, 2020, **2**, 146–157.
28 L. Yang, Y. Zou, W. Xia, H. Li, X. He, Y. Zhou, X. Liu, C. Zhang and Y. Li, *Nano Res.*, 2021, **14**, 969–975.
29 Z. Li, H. Li, J. Zhang, X. Liu, Z. Gu and Y. Li, *Chin. J. Polym. Sci.*, 2020, **738**, 1149–1156.
30 Z. Li, J. Zhang, Y. Fu, L. Yang, F. Zhu, X. Liu, Z. Gu and Y. Li, *J. Mater. Chem. B*, 2020, **8**, 7018–7023.
31 H. Wang, C. Wang, Y. Zou, J. Hu, Y. Li and Y. Cheng, *Giant*, 2020, **3**, 100022.
32 Y. Zou, X. Chen, W. Guo, X. Liu and Y. Li, *ACS Appl. Energy Mater.*, 2020, **3**, 2634–2642.
33 P. Yang, S. Zhang, X. Chen, X. Liu, Z. Wang and Y. Li, *Mater. Horiz.*, 2020, **7**, 746–761.
34 L. Yang, X. Guo, Z. Jin, W. Guo, G. Duan, X. Liu and Y. Li, *Nano Today*, 2021, **37**, 101075.
35 L. Yang, B. Gu, Z. Chen, Y. Yue, W. Wang, H. Zhang, X. Liu, S. Ren, W. Yang and Y. Li, *ACS Appl. Mater. Interfaces*, 2019, **11**, 30360–30367.
36 L. Su, Y. Yu, Y. Zhao, F. Liang and X. Zhang, *Sci. Rep.*, 2016, **6**, 24420.
37 L. Han, P. Li, P. Tang, X. Wang, T. Zhou, K. Wang, F. Ren, T. Guo and X. Lu, *Nanoscale*, 2019, **11**, 15846–15861.
38 Y. Ye, L. Zheng, T. Wu, X. Ding, F. Chen, Y. Yuan, G. C. Fan and Y. Shen, *ACS Appl. Mater. Interfaces*, 2020, **12**, 35626–35637.
39 H. Liu, X. Qu, H. Tan, J. Song, M. Lei, E. Kim, G. F. Payne and C. Liu, *Acta Biomater.*, 2019, **88**, 181–196.
40 Z. Li, X. Shan, Z. Chen, N. Gao, W. Zeng, X. Zeng and L. Mei, *Adv. Sci.*, 2020, **8**, 2002589.
41 Y. Fu, L. Liu, L. Zhang and W. Wang, *ACS Appl. Mater. Interfaces*, 2014, **6**, 5105–5112.
42 H. Karkhanechi, R. Takagi and H. Matsuyama, *Desalination*, 2014, **336**, 87–96.
43 Y. Zou, X. Chen, P. Yang, G. Liang, Y. Yang, Z. Gu and Y. Li, *Sci. Adv.*, 2020, **6**, eabb4696.
44 P. Yang, S. Zhang, N. Zhang, Y. Wang, J. Zhong, X. Sun, Y. Qi, X. Chen, Z. Li and Y. Li, *ACS Appl. Mater. Interfaces*, 2019, **11**, 42671–42679.
45 H.-W. Chien and T.-H. Chiu, *Eur. Polym. J.*, 2020, **130**, 109654.
46 M. M. Cowan, *Clin. Microbiol. Rev.*, 1999, **12**, 564–582.
47 C. Papuc, G. V. Goran, C. N. Predescu, V. Nicorescu and G. Stefan, *Compr. Rev. Food Sci. Food Saf.*, 2017, **16**, 1243–1268.
48 Z. Iqbal, E. P. C. Lai and T. J. Avis, *J. Mater. Chem.*, 2012, **22**, 21608.
49 J. Xu, K. Yao and Z. Xu, *Nanoscale*, 2019, **11**, 8680–8691.
50 W. Lei, K. Ren, T. Chen, X. Chen, B. Li, H. Chang and J. Ji, *Adv. Mater. Interfaces*, 2016, **3**, 21608.
51 X. Wang, L. Yang, P. Yang, W. Guo, Q. Zhang, X. Liu and Y. Li, *Sci. China Chem.*, 2020, **63**, 1295–1305.
52 A. J. Nappi and B. M. Christensen, *Insect Biochem. Mol. Biol.*, 2005, **35**, 443–459.
53 J. Song, H. Liu, M. Lei, H. Tan, Z. Chen, A. Antoshin, G. F. Payne, X. Qu and C. Liu, *ACS Appl. Mater. Interfaces*, 2020, **12**, 8915–8928.
54 Y. Fu, J. Zhang, Y. Wang, J. Li, J. Bao, X. Xu, C. Zhang, Y. Li, H. Wu and Z. Gu, *Carbohydr. Polym.*, 2021, **257**, 117598.
55 A. Dong, Y. J. Wang, Y. Gao, T. Gao and G. Gao, *Chem. Rev.*, 2017, **117**, 4806–4862.
56 C. Zhang, Y. Gu, G. Teng, L. Wang, X. Jin, Z. Qiang and W. Ma, *ACS Appl. Mater. Interfaces*, 2020, **12**, 29883–29898.
57 T. S. Sileika, H. D. Kim, P. Maniak and P. B. Messersmith, *ACS Appl. Mater. Interfaces*, 2011, **3**, 4602–4610.
58 S. He, P. Zhou, L. Wang, X. Xiong, Y. Zhang, Y. Deng and S. Wei, *J. R. Soc., Interface*, 2014, **11**, 20140169.
59 G. Yeroslavsky, O. Girshevitz, J. Foster-Frey, D. M. Donovan and S. Rahimipour, *Langmuir*, 2015, **31**, 1064–1073.
60 L. Guo, W. Yuan, Z. Lu and C. Li, *Colloids Surf., A*, 2013, **439**, 69–83.
61 C. Wu, G. Zhang, T. Xia, Z. Li, K. Zhao, Z. Deng, D. Guo and B. Peng, *Mater. Sci. Eng., C*, 2015, **55**, 155–165.
62 Q. Shi, H. Zhang, H. Zhang, P. Zhao, Y. Zhang and Y. Tang, *Sci. China Mater.*, 2020, **63**, 842–850.
63 M. Li, X. Liu, Z. Xu, K. W. Yeung and S. Wu, *ACS Appl. Mater. Interfaces*, 2016, **8**, 33972–33981.
64 H. Qian, J. Yang, Y. Lou, O. ur Rahman, Z. Li, X. Ding, J. Gao, C. Du and D. Zhang, *Appl. Surf. Sci.*, 2019, **465**, 267–278.
65 W. Li, W. Hu, Q. Liu, X. Liang, R. Chen, H. Ni and W. Zhan, *J. Mater. Sci.*, 2020, **55**, 9538–9550.
66 G. Liu, J. Xiang, Q. Xia, K. Li, H. Yan and L. Yu, *Ind. Eng. Chem. Res.*, 2020, **59**, 9666–9678.
67 Z. Liu and Y. Hu, *ACS Appl. Mater. Interfaces*, 2016, **8**, 21666–21673.
68 N. G. P. Chew, Y. Zhang, K. Goh, J. S. Ho, R. Xu and R. Wang, *ACS Appl. Mater. Interfaces*, 2019, **11**, 25524–25534.
69 M. S. Islam, N. Akter, M. M. Rahman, C. Shi, M. T. Islam, H. Zeng and M. S. Azam, *ACS Sustainable Chem. Eng.*, 2018, **6**, 9178–9188.
70 C. Gao, Y. Wang, F. Han, Z. Yuan, Q. Li, C. Shi, W. Cao, P. Zhou, X. Xing and B. Li, *J. Mater. Chem. B*, 2017, **5**, 9326–9336.
71 X. Xin, P. Li, Y. Zhu, L. Shi, J. Yuan and J. Shen, *Langmuir*, 2019, **35**, 1788–1797.
72 X. Liu, J. Chen, C. Qu, G. Bo, L. Jiang, H. Zhao, J. Zhang, Y. Lin, Y. Hua, P. Yang, N. Huang and Z. Yang, *ACS Biomater. Sci. Eng.*, 2018, **4**, 1568–1579.
73 Z. Jia, P. Xiu, S. I. Roohani-Esfahani, H. Zreiqat, P. Xiong, W. Zhou, J. Yan, Y. Cheng and Y. Zheng, *ACS Appl. Mater. Interfaces*, 2019, **11**, 4447–4469.
74 B. Shang, M. Xu, Z. Zhi, Y. Xi, Y. Wang, B. Peng, P. Li and Z. Deng, *J. Colloid Interface Sci.*, 2020, **558**, 47–54.
75 X. Xu, X. Liu, L. Tan, Z. Cui, X. Yang, S. Zhu, Z. Li, X. Yuan, Y. Zheng, K. W. K. Yeung, P. K. Chu and S. Wu, *Acta Biomater.*, 2018, **77**, 352–364.

76 Y. Cong, T. Xia, M. Zou, Z. Li, B. Peng, D. Guo and Z. Deng, *J. Mater. Chem. B*, 2014, **2**, 2450–3461.
77 A. GhavamiNejad, A. Rajan Unnithan, A. Ramachandra Kurup Sasikala, M. Samarikhalaj, R. G. Thomas, Y. Y. Jeong, S. Nasseri, P. Murugesan, D. Wu, C. Hee Park and C. S. Kim, *ACS Appl. Mater. Interfaces*, 2015, **7**, 12176–12183.
78 B. Wang, L. Zhao, W. Zhu, L. Fang and F. Ren, *Colloids Surf., B*, 2017, **157**, 432–439.
79 M. Li, Q. Liu, Z. Jia, X. Xu, Y. Shi, Y. Cheng and Y. Zheng, *J. Mater. Chem. B*, 2015, **3**, 8796–8805.
80 Y. Song, L. Cai, Z. Tian, Y. Wu and J. Chen, *ACS Omega*, 2020, **5**, 15083–15094.
81 Q. Xu, M. Chang, Y. Zhang, E. Wang, M. Xing, L. Gao, Z. Huan, F. Guo and J. Chang, *ACS Appl. Mater. Interfaces*, 2020, **12**, 31255–31269.
82 S. Kim, J.-M. Moon, J. S. Choi, W. K. Cho and S. M. Kang, *Adv. Funct. Mater.*, 2016, **26**, 4099–4105.
83 C. Ning, X. Wang, L. Li, Y. Zhu, M. Li, P. Yu, L. Zhou, Z. Zhou, J. Chen, G. Tan, Y. Zhang, Y. Wang and C. Mao, *Chem. Res. Toxicol.*, 2015, **28**, 1815–1822.
84 G. Yeroslavsky, M. Richman, L. O. Dawidowicz and S. Rahimipour, *Chem. Commun.*, 2013, **49**, 5721–5723.
85 G. Yeroslavsky, R. Lavi, A. Alishaev and S. Rahimipour, *Langmuir*, 2016, **32**, 5201–5212.
86 T. He, W. Zhu, X. Wang, P. Yu, S. Wang, G. Tan and C. Ning, *Mater. Technol.*, 2014, **30**, B68–B72.
87 L. Wang, X. Yang, W. Cao, C. Shi, P. Zhou, Q. Li, F. Han, J. Sun, X. Xing and B. Li, *RSC Adv.*, 2017, **7**, 51593–51604.
88 M. Li, L. Gao, C. Schlaich, J. Zhang, I. S. Donskyi, G. Yu, W. Li, Z. Tu, J. Rolff, T. Schwerdtle, R. Haag and N. Ma, *ACS Appl. Mater. Interfaces*, 2017, **9**, 35411–35418.
89 X. Li, P. Gao, J. Tan, K. Xiong, M. F. Maitz, C. Pan, H. Wu, Y. Chen, Z. Yang and N. Huang, *ACS Appl. Mater. Interfaces*, 2018, **10**, 40844–40853.
90 K. Ma, P. Dong, M. Liang, S. Yu, Y. Chen and F. Wang, *ACS Appl. Mater. Interfaces*, 2020, **12**, 6955–6965.
91 X. Xu, L. Wang, Z. Luo, Y. Ni, H. Sun, X. Gao, Y. Li, S. Zhang, Y. Li and S. Wei, *ACS Appl. Mater. Interfaces*, 2017, **9**, 43300–43314.
92 R. Wang, J. Li, W. Chen, T. Xu, S. Yun, Z. Xu, Z. Xu, T. Sato, B. Chi and H. Xu, *Adv. Funct. Mater.*, 2017, **27**, 1604894.
93 K. Patel, P. Kushwaha, S. Kumar and R. Kumar, *ACS Appl. Bio Mater.*, 2019, **2**, 5799–5809.
94 Z. Song, C. Niu, H. Wu, J. Wei, Y. Zhang and T. Yue, *ACS Appl. Mater. Interfaces*, 2019, **11**, 21874–21886.
95 C. Dhand, C. Y. Ong, N. Dwivedi, J. Varadarajan, M. Halleluyah Periayah, E. Jianyang Lim, V. Mayandi, E. T. L. Goh, R. P. Najjar, L. W. Chan, R. W. Beuerman, L. L. Foo, X. J. Loh and R. Lakshminarayanan, *ACS Biomater. Sci. Eng.*, 2020, **6**, 3162–3173.
96 T. Shen, W. Yang, X. Shen, W. Chen, B. Tao, X. Yang, J. Yuan, P. Liu and K. Cai, *ACS Biomater. Sci. Eng.*, 2018, **4**, 3211–3223.
97 G. Gao, Y. W. Jiang, H. R. Jia and F. G. Wu, *Biomaterials*, 2019, **188**, 83–95.
98 X. Wang, C. Wang, X. Wang, Y. Wang, Q. Zhang and Y. Cheng, *Chem. Mater.*, 2017, **29**, 1370–1376.
99 H.-H. Ran, X. Cheng, G. Gao, W. Sun, Y.-W. Jiang, X. Zhang, H.-R. Jia, Y. Qiao and F.-G. Wu, *ACS Appl. Bio Mater.*, 2020, **3**, 2438–2448.
100 D. He, T. Yang, W. Qian, C. Qi, L. Mao, X. Yu, H. Zhu, G. Luo and J. Deng, *Appl. Mater. Today*, 2018, **12**, 415–429.
101 C. Nie, C. Cheng, L. Ma, J. Deng and C. Zhao, *Langmuir*, 2016, **32**, 5955–5965.
102 M. Khamrai, S. L. Banerjee, S. Paul, A. K. Ghosh, P. Sarkar and P. P. Kundu, *ACS Sustainable Chem. Eng.*, 2019, **7**, 12083–12097.
103 Y. Liang, X. Zhao, T. Hu, Y. Han and B. Guo, *J. Colloid Interface Sci.*, 2019, **556**, 514–528.
104 H. Zhou, Y. Liu, W. Chi, C. Yu and Y. Yu, *Appl. Surf. Sci.*, 2013, **282**, 181–185.
105 S. Wang, C. Duan, W. Yang, X. Gao, J. Shi, J. Kang, Y. Deng, X. Shi and Z. Chen, *Nanoscale*, 2020, **12**, 11936–11946.
106 X. Ding, C. Yang, T. P. Lim, L. Y. Hsu, A. C. Engler, J. L. Hedrick and Y. Yang, *Biomaterials*, 2012, **33**, 6593–6603.
107 X. Jin, J. Yuan and J. Shen, *Colloids Surf., B*, 2016, **145**, 275–284.
108 L. Shi, W. Zhang, K. Yang, H. Shi, D. Li, J. Liu, J. Ji and P. K. Chu, *J. Mater. Chem. B*, 2015, **3**, 733–737.
109 L. Li, B. Yan, J. Yang, W. Huang, L. Chen and H. Zeng, *ACS Appl. Mater. Interfaces*, 2017, **9**, 9221–9225.
110 D. Gan, T. Xu, W. Xing, X. Ge, L. Fang, K. Wang, F. Ren and X. Lu, *Adv. Funct. Mater.*, 2019, **29**, 1805964.
111 D. Park, J. Kim, Y. M. Lee, J. Park and W. J. Kim, *Adv. Healthcare Mater.*, 2016, **5**, 2019–2024.
112 S. Yu, G. Li, R. Liu, D. Ma and W. Xue, *Adv. Funct. Mater.*, 2018, **28**, 1707440.
113 Z. Yuan, C. Lin, Y. He, B. Tao, M. Chen, J. Zhang, P. Liu and K. Cai, *ACS Nano*, 2020, **14**, 3546–3562.
114 S. Hong, J. Kim, Y. S. Na, J. Park, S. Kim, K. Singha, G. I. Im, D. K. Han, W. J. Kim and H. Lee, *Angew. Chem., Int. Ed.*, 2013, **52**, 9187–9191.
115 Z. Sadrearhami, F. N. Shafiee, K. K. K. Ho, N. Kumar, M. Krasowska, A. Blencowe, E. H. H. Wong and C. Boyer, *ACS Appl. Mater. Interfaces*, 2019, **11**, 7320–7329.
116 J. H. Ryu, P. B. Messersmith and H. Lee, *ACS Appl. Mater. Interfaces*, 2018, **10**, 7523–7540.
117 X. Wang, Z. Chen, P. Yang, J. Hu, Z. Wang and Y. Li, *Polym. Chem.*, 2019, **10**, 4194–4200.
118 I. S. Kwon and C. J. Bettinger, *J. Mater. Chem. B*, 2018, **6**, 6895–6903.
119 L. Bouarab-Chibane, V. Forquet, P. Lanteri, Y. Clement, L. Leonard-Akkari, N. Oulahal, P. Degraeve and C. Bordes, *Front. Microbiol.*, 2019, **10**, 829.
120 Y. Peng, J. Nie, W. Cheng, G. Liu, D. Zhu, L. Zhang, C. Liang, L. Mei, L. Huang and X. Zeng, *Biomater. Sci.*, 2018, **6**, 1084–1098.
121 Y. Liang, X. Zhao, T. Hu, B. Chen, Z. Yin, P. X. Ma and B. Guo, *Small*, 2019, **15**, 1900046.

 

122 M. Yin, Y. Wang, Y. Zhang, X. Ren, Y. Qiu and T. Huang, *Carbohydr. Polym.*, 2020, **232**, 115823.
123 S. K. Madhurakkat Perikamana, J. Lee, Y. B. Lee, Y. M. Shin, E. J. Lee, A. G. Mikos and H. Shin, *Biomacromolecules*, 2015, **16**, 2541–2555.
124 X. Zhang, Z. Li, P. Yang, G. Duan, X. Liu, Z. Gu and Y. Li, *Mater. Horiz.*, 2021, **8**, 145–167.
125 S. Mei, X. Xu, R. D. Priestley and Y. Lu, *Chem. Sci.*, 2020, **11**, 12269–12281.
126 N. Pandey, L. F. Soto-Garcia, J. Liao, Z. Philippe, K. T. Nguyen and Y. Hong, *Biomater. Sci.*, 2020, **8**, 1240–1255.
127 N. A. O'Connor, A. Syed, M. Wong, J. Hicks, G. Nunez, A. Jitianu, Z. Siler and M. Peterson, *Gels*, 2020, **6**, 39.